

**Low temperature HD + *ortho*-/*para*-H<sub>2</sub> inelastic scattering of astrophysical interest**Renat A. Sultanov<sup>1,2a),1</sup>, Dennis Guster<sup>2b)</sup>, and S. K. Adhikari<sup>1c)</sup>

<sup>1)</sup>*Instituto de Física Teórica, UNESP – Universidade Estadual Paulista, 01140 São Paulo, SP, Brazil*

<sup>2)</sup>*Department of Information Systems, BCRL & Integrated Science and Engineering Laboratory Facility (ISELF) at St. Cloud State University, St. Cloud, MN, USA*

(Dated: 20 July 2018)

State-selected total cross sections and thermal rate coefficients are computed for the HD + *ortho*-/*para*-H<sub>2</sub> rotational energy transfer collision at low temperatures: 2 K  $\lesssim$  T  $\lesssim$  300 K. A modified H<sub>2</sub>-H<sub>2</sub> potential energy surface (PES) devised by Hinde is used for this pure quantum-mechanical dynamical computation. A comparison of the new results for the HD + *ortho*-/*para*-H<sub>2</sub> scattering problem and previous calculations computed with the use of other older PESs is presented and discussed.

PACS numbers: 36.10.Dr

---

<sup>a)</sup> Electronic mail: [rasultanov@stcloudstate.edu](mailto:rasultanov@stcloudstate.edu); [r.sultanov2@yahoo.com](mailto:r.sultanov2@yahoo.com)

<sup>b)</sup> Electronic mail: [dcguster@stcloudstate.edu](mailto:dcguster@stcloudstate.edu)

<sup>c)</sup> Electronic mail: [adhikari@ift.unesp.br](mailto:adhikari@ift.unesp.br); <http://www.ift.unesp.br/users/adhikari>

## I. INTRODUCTION

Elastic and inelastic collisions between atoms and molecules and/or between molecules and molecules are of great scientific interest in the fields of physical-chemistry and chemical-physics. The reason is that such processes can provide valuable information about fundamental interactions between different chemical species, their chemical properties, their energy transfer quantum dynamics and many other properties. The pioneering studies focussed on light atoms and molecules, because of their simple nature. For three- and four-atomic systems with a small number of electrons, the potential energy surface (PES) can be computed with relatively high accuracy<sup>1-6</sup>. Consequently, for these systems one can then more easily test different dynamical methods, such as, classical, semi-classical, quasi-classical trajectory, and pure quantum-mechanical computational formulations and compare the results with available experimental data in a controlled fashion. The test methods devised could then be applied to more complex many-atomic systems, wherein a controlled comparison is not possible. Among these small systems the four-atomic  $\text{H}_2+\text{H}_2$  and  $\text{H}_2+\text{HD}$  scattering processes have attracted significant attention not only in chemical physics but also in astrophysics. In astrophysics  $\text{H}_2$  and HD play an important role, because of their abundance in the molecular cloud of the universe<sup>7,8</sup>. Together with the  $\text{H}_2 + \text{H}_2$  collision, the  $\text{HD} + \text{H}_2$  collision is also of significant importance in the astrophysics of the early universe. Specifically it is important in the modeling of pre-galactic clouds and planetary atmospheres; in the cooling of primordial gas and in the formation of stars<sup>9-15</sup>.

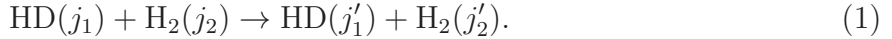
In Ref.<sup>16</sup> a semiclassical treatment of  $\text{H}_2\text{-H}_2$  scattering is formulated. In Ref.<sup>17</sup> the author developed and applied a rigid rotor model to study rotational excitation in  $\text{H}_2\text{-H}_2$  by applying quantum close-coupling scattering calculations. In this approach the distance between the hydrogen atoms in both  $\text{H}_2$  molecules was fixed at a constant value based on average. This model was applied to many different atomic and molecular systems, see, for example<sup>13,18-20</sup>. The main goal of the work<sup>17</sup> was to compute rotational thermal rate coefficients in the  $\text{H}_2+\text{H}_2$  system at low temperatures of astrophysical interest. Quantum-mechanical close-coupling calculations for three-dimensional collisions of *para*- $\text{H}_2$  and *ortho*- $\text{H}_2$  with HD are performed in Ref.<sup>11,13,18,19,21</sup>, where the HD- $\text{H}_2$  potential is derived from the  $\text{H}_2\text{-H}_2$  potential. A quantum dynamical study of  $\text{H}_2\text{-H}_2$  collisions is reported for both *ortho*- and *para*- $\text{H}_2$  in Refs.<sup>22-24</sup>. In Ref.<sup>25</sup>, the authors considered  $\text{H}_2+\text{H}_2$  and  $\text{D}_2+\text{D}_2$  rotational inelastic scat-

terings with the use of the H<sub>2</sub>-H<sub>2</sub> potential energy surface (PES) from Ref.<sup>1</sup>. In Ref.<sup>22,26</sup> a full six-dimensional scattering computation has been performed taking into account vibrational relaxation in the H<sub>2</sub>+H<sub>2</sub> collision. In that study the H<sub>2</sub>-H<sub>2</sub> PES from Ref.<sup>2</sup> was used and its anisotropy properties have been studied at low temperatures: 20 K  $\lesssim$  T  $\lesssim$  300 K. HD+HD scattering has been studied experimentally in Ref.<sup>27</sup> and theoretically in<sup>28</sup> for a wide range of collision energies. A comprehensive computational and experimental study of total cross section in H<sub>2</sub>-H<sub>2</sub>, D<sub>2</sub>-D<sub>2</sub>, and HD-HD scattering for both ortho and para H<sub>2</sub> and D<sub>2</sub> has been reported in Ref.<sup>29</sup>. Measurements of energy transfer rates in HD+HD<sup>30</sup> and H<sub>2</sub>+H<sub>2</sub><sup>31,32</sup> collisions have also been performed.

However, realistic theoretical investigations of the low-energy HD+H<sub>2</sub> collision are lacking, although preliminary quantum calculation of this process has been reported in Refs.<sup>11,13</sup>. Schaefer<sup>11</sup> calculated rate coefficients for the excitation of HD by H<sub>2</sub>, for the low-lying rotational levels using a modified older potential for HD and H<sub>2</sub>. Flower<sup>13</sup> performed an improved calculation of HD-H<sub>2</sub> scattering with Schwenke's H<sub>2</sub>-H<sub>2</sub> PES using a larger rotational basis set<sup>3</sup>. In this paper we report an improved calculation of this problem using a realistic HD-H<sub>2</sub> PES derived from Hinde's recent H<sub>2</sub>-H<sub>2</sub> PES<sup>5</sup>. In two papers<sup>18,19</sup> the PES from work<sup>2</sup> has been applied together with a pure quantum-mechanical dynamical approach. The surprising thing is, that the results of works<sup>18,19</sup> are closer to the results of older work<sup>11</sup> than to<sup>13</sup>. Therefore, there is a need to carry out new computations with newer PES between HD and H<sub>2</sub>.

While the exchange symmetry is broken in HD+H<sub>2</sub> it still possesses many similarities with the H<sub>2</sub>+H<sub>2</sub> system. The PESs of H<sub>2</sub>-H<sub>2</sub> and HD-H<sub>2</sub> should basically be the same six-dimensional function. This fact follows from the general Born-Oppenheimer approach<sup>33</sup>. At the same time the two collisions: H<sub>2</sub>+H<sub>2</sub> and H<sub>2</sub>+HD, should have rather different scattering outputs. This is because the H<sub>2</sub> and HD molecules have fairly different rotational constants, internal symmetries and as a result a different rotational-vibrational spectrum. The HD-H<sub>2</sub> PES can be derived from the H<sub>2</sub>-H<sub>2</sub> PES by shifting the center of mass (c.m.) of the H<sub>2</sub> molecule to the c.m. of the HD molecule. Once the exchange symmetry is broken in H<sub>2</sub>-H<sub>2</sub> by replacing the H with the D atom in one of the H<sub>2</sub>'s then one has the new HD-H<sub>2</sub> PES. In this fashion, we constructed the HD-H<sub>2</sub> PES from the H<sub>2</sub>-H<sub>2</sub> PES of Hinde<sup>5</sup> employing all parts of the full HD-H<sub>2</sub> interaction including the HD's dipole moment. Using this HD-H<sub>2</sub> PES we carried out pure quantum-mechanical calculations for inelastic collisions of rotationally

excited HD and H<sub>2</sub> molecules, i.e. the process:



The scattering cross sections and their corresponding thermal rate coefficients are computed using a non-reactive quantum-mechanical close-coupling approach. The four-atomic system is shown in Fig. 1.

In Sec. II we briefly describe the quantum-mechanical approach used in this paper. Sec. III includes the computational results. We compare the cross-sections and rates with those of other authors<sup>11,13</sup>, and our previous calculations<sup>18,19</sup>, where a different HD-H<sub>2</sub> PES, derived from the well-known Boothroyd-Martin-Keogh-Peterson (BMKP) H<sub>2</sub>-H<sub>2</sub> PES<sup>2</sup>, was used. Discussion and conclusions are provided in Sec. IV. The corresponding procedure to obtain a modified HD-H<sub>2</sub> PES from the existing H<sub>2</sub>-H<sub>2</sub> surface<sup>5</sup> is presented in Sec. V. Atomic units ( $e = m_e = \hbar = 1$ ) are used throughout this paper.

## II. QUANTUM-MECHANICAL APPROACH

In this section we provide a brief account of the present quantum-mechanical close-coupling approach following the method in Ref.<sup>17</sup>. The HD and H<sub>2</sub> molecules are treated as linear rigid rotors. The model has been applied in few previous works<sup>13,17</sup>. In all our calculations with this potential the bond length was fixed at 1.449 a.u. or 0.7668 Å for the H<sub>2</sub> molecule and 1.442 a.u. for HD which is 0.7631 Å. The Schrödinger equation for the (12) + (34) collision in the c.m. frame, where (12) and (34) are diatomic molecules formed by atoms 1-4 is<sup>17</sup>:

$$\left[ \frac{\hat{P}_{\vec{R}_3}^2}{2\mathcal{M}_{12}} + \frac{\hat{L}_{\vec{R}_1}^2}{2\mu_1 R_1^2} + \frac{\hat{L}_{\vec{R}_2}^2}{2\mu_2 R_2^2} + V(\vec{R}_1, \vec{R}_2, \vec{R}_3) - E \right] \Psi(\hat{R}_1, \hat{R}_2, \vec{R}_3) = 0. \quad (2)$$

Here  $\hat{P}_{\vec{R}_3}$  is the momentum operator of the kinetic energy of the collision,  $\vec{R}_3$  is the collision coordinate, whereas  $\vec{R}_1$  and  $\vec{R}_2$  are relative vectors between atoms in the two diatomic molecules as shown in Fig. 1, and  $\hat{L}_{\vec{R}_{1(2)}}$  are the quantum-mechanical rotation operators of the rigid rotors,  $\mu_1$  and  $\mu_2$  are the reduced masses of the HD and H<sub>2</sub> molecules and  $\mathcal{M}_{12}$  is the reduced mass of the two molecules. The vectors  $\hat{R}_{1(2)}$  are the angles of orientation for rotors (12) and (34), respectively;  $V(\vec{R}_1, \vec{R}_2, \vec{R}_3)$  is the PES of the four-atomic system (1234), and  $E$  is the total energy in the c.m. system. The use and modification of the original H<sub>2</sub>-H<sub>2</sub>

PESs  $V(\vec{R}_1, \vec{R}_2, \vec{R}_3)$  is discussed in Appendix A, i.e. Sec. 5. The cross sections for rotational excitation and relaxation can be obtained from the  $S$ -matrix  $S_{\alpha\alpha'}^J$ . The cross sections for excitation from  $\text{HD}(j_1, m_1) + \text{H}_2(j_2, m_2)$  to  $\text{HD}(j'_1 m'_1) + \text{H}_2(j'_2 m'_2)$  are summed over the final angular momentum projections  $(m'_1 m'_2)$  and averaged over the initial projections  $(m_1 m_2)$  of the HD and H<sub>2</sub> molecules of angular momenta  $j_1$  and  $j_2$  are given by:

$$\sigma(j'_1, j'_2; j_1 j_2, \varepsilon) = \frac{\pi}{(2j_1 + 1)(2j_2 + 1)k_{\alpha\alpha'}} \sum_{J j_{12} j'_{12} L L'} (2J + 1) |\delta_{\alpha\alpha'} - S_{\alpha\alpha'}^J(E)|^2. \quad (3)$$

The kinetic energy is  $\varepsilon = E - B_1 j_1(j_1 + 1) - B_2 j_2(j_2 + 1)$ , where  $B_1 = 44.7 \text{ cm}^{-1}$  and  $B_2 = 60.8 \text{ cm}^{-1}$  are the rotation constants of rigid rotors (12) and (34) respectively, they are shown in Fig. 1. Next,  $E$  is the total energy of the system,  $J$  is total angular momenta of the four-atomic system,  $\alpha \equiv (j_1 j_2 j_{12} L)$ , where  $j_1 + j_2 = j_{12}$  and  $j_{12} + L = J$ ,  $k_{\alpha\alpha'} = \sqrt{2\mathcal{M}_{12}(E + E_\alpha - E_{\alpha'})}$  is the channel wavenumber and  $E_{\alpha(\alpha')}$  are rotational channel energies. Finally, the relationship between the rotational thermal-rate coefficient  $k_{j_1 j_2 \rightarrow j'_1 j'_2}(T)$  at temperature  $T$  and the corresponding cross section  $\sigma_{j_1 j_2 \rightarrow j'_1 j'_2}(\varepsilon)$ , can be obtained through the following weighted average formula:

$$k_{j_1 j_2 \rightarrow j'_1 j'_2}(T) = \sqrt{\frac{8k_B T}{\pi \mathcal{M}_{12}}} \frac{1}{(k_B T)^2} \int_{\varepsilon_s}^{\infty} \sigma_{j_1 j_2 \rightarrow j'_1 j'_2}(\varepsilon) e^{-\varepsilon/k_B T} \varepsilon d\varepsilon, \quad (4)$$

where  $k_B$  is Boltzman constant and  $\varepsilon = E - E_{j_1} - E_{j_2}$  is pre-collisional translational energy at the translational temperature  $T$ ,  $k_B$  is Boltzmann constant and  $\varepsilon_s$  is the minimum kinetic energy for the levels  $j_1$  and  $j_2$  to become accessible.

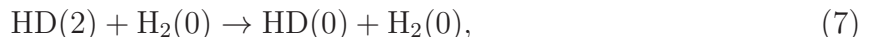
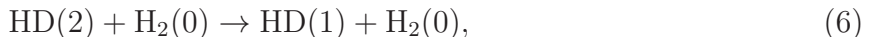
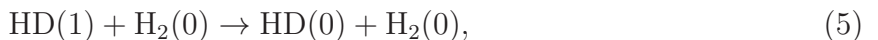
### III. NUMERICAL RESULTS

We used the MOLSCAT program<sup>34</sup> to solve the Schrödinger Eq.(2). Convergence was obtained for the integral cross sections,  $\sigma(j'_1, j'_2; j_1 j_2, \varepsilon)$ , with respect to the variation of the variables utilized in all considered collisions at different collision energies. For the intermolecular distance  $R_3$  we used from  $R_{3min} = 3.0$  a.u. to  $R_{3max} = 30.0$  a.u. We also applied a few different propagators included in the MOLSCAT computer program, and our calculation show that D. Manolopoulos's hybrid modified log-derivative propagator technique<sup>35</sup> would be quite numerically stable and a time effective approach. This method is used in the majority of the calculations.

The maximum value of the total angular momentum  $J$  was set at 44 while the number of levels  $N_{lvl}$  in the basis set of HD + H<sub>2</sub> was set at 42. Specifically, in the case of HD( $j_1$ )+*para*-H<sub>2</sub>( $j_2$ ),  $j_1$  it has values 0, 1, 2, and 3 and  $j_2$  has values 0, 2, and 4. This combination generates the total number of included levels  $N_{lvl}=34$ . In the case of HD+*ortho*-H<sub>2</sub> the parameter  $j_1$  has values 0, 1, 2, and 3 and  $j_2$  has values 1, 3, and 5. This results in the total number of levels  $N_{lvl}=42$ . A number of test computations with higher values for the  $j_1$  and  $j_2$  parameters have been carried out. For example, in the case of HD+*para*-H<sub>2</sub>,  $j_1$  was taken as 0, 1, 2, 3, 4 and  $j_2$  as 0, 2, 4, 6. This  $j_1/j_2$  combination produced  $N_{lvl} = 74$ . We obtained similar results in both cases, confirming the convergence of the calculations.

Because the HD+H<sub>2</sub> total rotational energy transfer cross sections (3) has shape resonances at low energies a large number of energy points are needed in order to effectively reproduce them. We used up to 250 energy points in each computation for each specific rotational transition in the HD and H<sub>2</sub> molecules considered. More space discretization points were used at low collision energies and fewer points in the higher-energy sector.

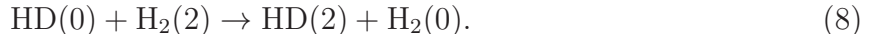
Below we present results for cross sections and thermal rate coefficients for different quantum-state transitions in HD and H<sub>2</sub> molecules. We reproduced shape resonances in the low velocity region, which are very important in the cooling of the astrophysical media at low temperatures. We compared them with the older quantum-dynamical results of Schaefer<sup>11</sup> and Flower<sup>13</sup>. We also present results<sup>18,20</sup> using a PES obtained from a modification of the BMKP H<sub>2</sub>-H<sub>2</sub> PES<sup>2</sup>, viz. Sec. V (Appendix A). In Figs. 2,3 and 4 we show four different results for the integral cross sections in the collisions:



respectively. One can see that the new cross sections obtained with the present PES have the same structure and shape, but also have substantially larger ( $\sim 60\%$ ) values at medium energies ( $v > 200$  m/sec) when compared with the results obtained from the modified BMKP PES<sup>2</sup> and the older result from Schaefer's calculations<sup>11</sup>. Processes (6) and (7) are also important collisions from the astrophysical point of view. They represent transitions from the  $j_1 = 2$  and  $j_2 = 0$  state of the HD( $j_1$ )+H<sub>2</sub>( $j_2$ ) system. It is seen from Table I that the corresponding rotational energy of the system is 268.2 cm<sup>-1</sup> and rotational relaxation

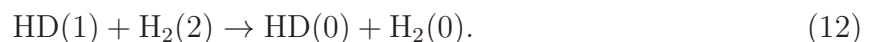
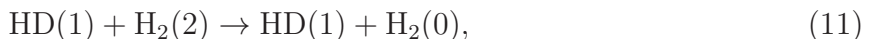
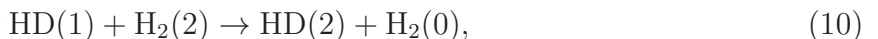
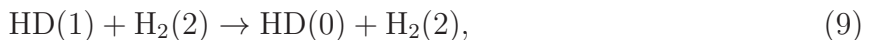
processes to states of lower energy should be relevant. The cross sections from Ref.<sup>13</sup> are available only for higher collision velocities, i.e.  $v \geq 300$  m/s. The present cross sections have the same behavior as previous results, but they have larger values than the old ones, specially at higher energies. Next in Fig. 5 we exhibit the thermal rate coefficients corresponding to the processes considered above. Here, we additionally include the older results from Ref.<sup>13</sup>, where Schwenke's H<sub>2</sub>-H<sub>2</sub> PES<sup>3</sup> was used. One can see that the new rates are substantially larger than those of other calculations. In general, it means that the contribution of the HD+H<sub>2</sub> collision to the HD-cooling function can have even larger contributions than previously expected.

Now we consider the inelastic cross sections in HD+H<sub>2</sub> for higher rotational energies. For the systems HD(0)+H<sub>2</sub>(2) and HD(1)+H<sub>2</sub>(2), one can see from Table I that the corresponding rotational energies are 364.8 cm<sup>-1</sup> and 454.2 cm<sup>-1</sup>. In Fig. 6 (upper plot) we show the integral cross sections for the process:



While we obtain a relatively good agreement between cross sections calculated with the older modified BMKP PES and Hinde's PES, there is a dramatic difference with the corresponding result from Ref.<sup>11</sup>. The present cross sections are larger than those of Ref.<sup>11</sup> by a few orders of magnitude. In Fig. 6 (lower plot) we show the results for the corresponding thermal rate coefficient  $k_{20 \rightarrow 02}(T)$ . It is seen, that the present rates and those obtained by Flower<sup>13</sup> have a flat temperature dependence, whereas the rate of Schaefer<sup>11</sup>, although smaller than other results, increases monotonically with energy. Because the thermal rate of reaction (8) is relatively large, one can conclude that this channel can also make a substantial contribution to the astrophysical HD-cooling function.

In Figs. 7-10 we show results for the total cross section in the inelastic scattering from the state HD(1) + H<sub>2</sub>(2) with rotational energy 454.2 cm<sup>-1</sup>, viz. Table I. All de-excitation processes have been computed for this state, namely:



The present cross sections exhibit fairly good agreement with the results computed with the modified BMKP PES<sup>2</sup>, and also with older results from Ref.<sup>11</sup>. The general shape and trend of the behavior of these cross sections are the same in all cases. Also, there is a relatively small bump in the cross sections of the processes (10)-(12) at collision velocity  $\sim 1100$  m/sec which is also reproduced by two PESs. One can see that the process (9) can make a significant contribution to the total HD-cooling function because its cross section is rather large relative to other channels. Finally, in order to carry out new computations of the astrophysical cooling function, Table II includes the relevant thermal rate coefficients for the HD + *para*-H<sub>2</sub> case in the temperature range from 2 K to 300 K. Next, as a test, we choose the initial state HD(2) + H<sub>2</sub>(2) with a relatively higher total rotational energy: 633 cm<sup>-1</sup>. The integral de-excitation cross sections from this state to different lower energy rotational states are shown in Fig. 11. One can see a fairly good agreement in the shape of the curves between various rotational transition results for the integral cross sections computed with the two different PESs.

In Fig. 12 we show three different rotational transition cross-sections for the *ortho*-hydrogen case. Here we chose low lying rotational levels of the two molecules: HD(1) + H<sub>2</sub>(1) and HD(2) + H<sub>2</sub>(1). Some results from older works<sup>11,13,19</sup> are also presented in the figure together with results computed with the newer modified PES from<sup>5</sup>. The corresponding thermal rate coefficients are shown in Fig. 13 where the older results from Refs.<sup>11,13,19</sup> are also presented for comparison purposes. Figures 14 and 15 include results for thermal rate coefficients for the transitions from higher rotational states, e.g., HD(0) + H<sub>2</sub>(3) and HD(1) + H<sub>2</sub>(3).

Finally, in Sec. VI (Appendix B) we present our new results for the thermal rate coefficients which can be used in subsequent computation of the astrophysical HD-cooling function. In Table II we show thermal rates of different de-excitation processes in low-temperature HD + *para*-H<sub>2</sub> rotational energy transfer collisions and in Table III the same data for the HD + *ortho*-H<sub>2</sub> case.

#### IV. SUMMARY AND CONCLUSIONS

State-to-state close-coupling quantum-mechanical calculations for rotational de-excitation cross-sections and corresponding thermal rate coefficients of the HD+*o/p*-H<sub>2</sub> collisions are



presented using a linear rigid rotor model for the HD and H<sub>2</sub> molecules. The symmetrical H<sub>2</sub>-H<sub>2</sub> PES of Ref.<sup>5</sup> has been appropriately adopted for the current non-symmetrical HD+H<sub>2</sub> system by appropriate translation and rotation. These geometrical operations lead to a new set of angle variables  $\theta'_1, \theta'_2$  and  $\varphi'_2$  for the Jacobi few-body coordinates, a new length of the intermolecular distance  $\vec{R}'_3$  and, as a result, to a new HD-H<sub>2</sub> PES. For comparison purposes in this paper we carried out a few calculations with the use of the older BMKP PES<sup>2</sup> which was also modified for HD-H<sub>2</sub>. A test of convergence and the results for the cross-sections with the two PESs are obtained for a wide range of values of different parameters. It is seen from Figs. 2, 3 and 4, that in most cases for the lower number quantum transition states the rotational energy transfer cross sections obtained with the use of the modified Hinde's PES have higher values than the cross sections computed with the use of the modified BMKP PES<sup>18,19</sup>. The same situation occurs in comparisons within the older work<sup>11</sup>. In Fig. 5 the corresponding thermal rate coefficients are presented. In this case we include results from the paper<sup>13</sup> too. As can be seen the new thermal rates (solid lines) have substantially higher values than the other results. For example, in the rotational energy transfer, process (5), new thermal rates are  $\sim 2$  times higher than the other corresponding rates. Because (5) is considered as one of the main contributors to the resulting HD cooling process, one can say that the new HD-cooling function may have substantially greater values than the previous calculations<sup>12</sup>. Next, Fig. 6 represents results for a very interesting process (8). The interest in this channel lies in the fact that both molecules change their rotational quantum numbers by  $\Delta j=2$ , therewith HD becomes excited and H<sub>2</sub> de-excited. In this case we obtained a significant deviation from the results of work<sup>11</sup>. However, the cross sections obtained with the modified versions of the Hinde and BMKP PESs are fairly close to each other and have fairly large values. Therefore, this process probably can make a contribution to the HD cooling process. In addition we would like to note, that in work<sup>12</sup> the process has also been computed and discussed, in which significant differences from<sup>11</sup> were also found.

Further, the following four Figs. (7)-(10) represent our integral cross sections and corresponding results from work<sup>11</sup> for the following de-excitation collisions: (9), (10), (11), and (12). In all of these processes the initial state of HD has the rotational state  $j_1=1$  and H<sub>2</sub> has the rotational state  $j_2=2$ . The corresponding total rotational energy of the molecules can be found in Table I. The results in Fig. (7) are in fairly good agreement with each other and have relatively large values, therefore this specific channel could also make a substantial

contribution to the cooling function. It was found, that in Figs. (8)-(10) both surfaces, namely, Hinde's and BMKP both accurately reproduce the position of a shape resonance at collision velocity  $v \sim 1300$  m/sec. Fig. 11 shows the resulting de-excitation cross sections from the highly located rotational quantum level. Finally, our analysis in this paper would not be complete if we did not undertake computations for the *ortho* hydrogen case as well. Fig. 12 shows results for the lower lying rotational quantum numbers of HD, namely,  $j_1=0$  and 1, and  $H_2: j_2=1$ . It is seen that in this case the cross sections obtained with the Hinde PES are significantly larger than other results. The corresponding thermal rate coefficients are presented in Fig. 13. Again, as in previous *para*-hydrogen cases the new rates obtained with Hinde's potential are larger than previous results. At the low density limit and taking into account the critical density concept the total cooling function can be computed with the use of the following formula:

$$\Lambda_{\text{HD}}(T) = \sum_{j_1 j_2, j'_1 j'_2} n_{\text{HD}}(j_1) n_{\text{H}_2}(j_2) k_{j_1 j_2 \rightarrow j'_1 j'_2}(T) h\nu_{j_1 j_2 \rightarrow j'_1 j'_2}, \quad (13)$$

which is in units of  $[\text{erg} \times \text{cm}^{-3} \times \text{s}^{-1}]$ . Here,  $h\nu_{j_1 j_2 \rightarrow j'_1 j'_2}$  is the emitted photon energy,  $k_{j_1 j_2 \rightarrow j'_1 j'_2}(T)$  is the thermal rate coefficient (4) corresponding to the rotational transitions  $j_1 j_2 \rightarrow j'_1 j'_2$ . Therefore, increasing the knowledge of rotational and possibly vibrational excitation and de-excitation rate constants,  $k_{jv \rightarrow j'v'}(T)$ , in atomic and molecular hydrogen-hydrogen collisions, such as HD/ $H_2+H_2$ , HD/ $H_2+H$  etc, is important in order to understand and be able to model the energy balance in the interstellar medium. For comparison purposes it would be very useful and interesting to carry out new computations of the rotational-vibrational integral cross sections and corresponding thermal rate coefficients for a low-energy HD+H collision. In this case a different  $H_3$  PESs from papers<sup>43,44</sup> could be applied.

## ACKNOWLEDGMENTS

This paper was supported by the Office of Research and Sponsored Programs of St. Cloud State University, USA and CNPq and FAPESP of Brazil.

## V. APPENDIX A: HD-H<sub>2</sub> POTENTIAL ENERGY SURFACES

A few important modifications to the Hinde H<sub>2</sub>-H<sub>2</sub> PES<sup>5</sup> were needed for the current non-symmetrical four-atomic collision (1). The application and modification of the original H<sub>2</sub>-H<sub>2</sub> BMKP PES were published in Ref.<sup>18</sup>. Below in this paragraph we briefly describe the procedure. To compute the distances between the four atoms the BMKP PES uses Cartesian coordinates. Consequently, it was necessary to convert spherical coordinates used in the close-coupling method to the corresponding Cartesian coordinates and compute the distances between the four atoms followed by calculation of the PES<sup>18,19</sup>. This procedure used a specifically oriented coordinate system  $OXYZ$ . As a first step we needed to introduce the Jacobi coordinates  $\{\vec{R}_1, \vec{R}_2, \vec{R}_3\}$  and the radius-vectors of all four atoms in the space-fixed coordinate system  $OXYZ$ :  $\{\vec{r}_1, \vec{r}_2, \vec{r}_3, \vec{r}_4\}$ . Then the center of mass of the HD molecule has been relocated at the origin of the coordinate system  $OXYZ$ , and the  $\vec{R}_3$  was directed to center of mass of the H<sub>2</sub> molecule along the  $OZ$  axis. Thus, one could obtain the following coordinate relationships:  $\vec{R}_3 = \{R_3, \Theta_3 = 0, \Phi_3 = 0\}$ , with  $\Theta_3$  and  $\Phi_3$  the polar and azimuthal angles,  $\vec{R}_1 = \vec{r}_1 - \vec{r}_2$ ,  $\vec{R}_2 = \vec{r}_4 - \vec{r}_3$ ,  $\vec{r}_1 = \xi\vec{R}_1$  and  $\vec{r}_2 = (1 - \xi)\vec{R}_1$ , where  $\xi = m_2/(m_1 + m_2)$ <sup>18</sup>. Further, we adopted the  $OXYZ$  system in such a way, that the HD inter-atomic vector  $\vec{R}_1$  lies on the  $XOZ$  plane. Then the angle variables of  $\vec{R}_1$  and  $\vec{R}_2$  are:  $\hat{R}_1 = \{\Theta_1, \Phi_1 = \pi\}$  and  $\hat{R}_2 = \{\Theta_2, \Phi_2\}$  respectively. One can see, that the Cartesian coordinates of the atoms of the HD molecule are<sup>18</sup>:  $\vec{r}_1 = \{x_1 = \xi R_1 \sin \Theta_1, y_1 = 0, z_1 = \xi R_1 \cos \Theta_1\}$ ,  $\vec{r}_2 = \{x_2 = -(1 - \xi)R_1 \sin \Theta_1, y_2 = 0, z_2 = -(1 - \xi)R_1 \cos \Theta_1\}$ . Defining  $\zeta = m_4/(m_3 + m_4)$ , we have  $\vec{r}_3 = \vec{R}_3 - (1 - \zeta)\vec{R}_2$ ,  $\vec{r}_4 = \vec{R}_3 + \zeta\vec{R}_2$ , and the corresponding Cartesian coordinates are:  $\vec{r}_3 = \{x_3 = -(1 - \zeta)R_2 \sin \Theta_2 \cos \Phi_2, y_3 = -(1 - \zeta)R_2 \sin \Theta_2 \sin \Phi_2, z_3 = R_3 - (1 - \zeta)R_2 \cos \Theta_2\}$ ,  $\vec{r}_4 = \{x_4 = \zeta R_2 \sin \Theta_2 \cos \Phi_2, y_4 = \zeta R_2 \sin \Theta_2 \sin \Phi_2, z_4 = R_3 + \zeta R_2 \cos \Theta_2\}$ . In such a manner the cartesian and the Jacobi coordinates are represented together for the four-atomic system HD+H<sub>2</sub><sup>18</sup>.

The Hinde H<sub>2</sub>-H<sub>2</sub> PES<sup>5</sup> is a six-dimensional surface which was constructed using recent Raman spectrum data of the (H<sub>2</sub>)<sub>2</sub> dimer and which accurately describes the dimer's van der Waals well<sup>5</sup>. It was demonstrated that this PES gives IR and Raman transition energies for the (*para*-H<sub>2</sub>)<sub>2</sub>, (*ortho*-D<sub>2</sub>)<sub>2</sub>, and (*para*-H<sub>2</sub>)-(*ortho*-D<sub>2</sub>) dimers and is in good agreement with experimental data.

The method to make the Hinde H<sub>2</sub>-H<sub>2</sub> PES suitable for the non-symmetric system HD+H<sub>2</sub>

is based on a geometrical transformation technique, i.e. a rotation of the three-dimensional space and the corresponding space-fixed coordinate system  $OXYZ$ . The new global PES depends on six variables (Jacobi coordinates) –  $|\vec{R}_1|$ ,  $|\vec{R}_2|$ ,  $|\vec{R}_3|$ ,  $\theta_1$ ,  $\theta_2$ , and  $\varphi_2$  – as shown in Fig. 1 together with corresponding quantum angular momenta. The initial geometry of the system is designed in such a way that the Jacobi vector  $\vec{R}_3$  connects the c.m.'s of the two  $H_2$  molecules and is directed over the  $OZ$  axis. We laid out  $OXYZ$  in such a manner that the Jacobi vector  $\vec{R}_1$  lies in the  $XOZ$  plane. The vector  $\vec{R}_2$  can then be directed anywhere. The spherical coordinates of the Jacobi vectors are:  $\vec{R}_1 = \{R_1, \theta_1, 0\}$ ,  $\vec{R}_2 = \{R_2, \theta_2, \varphi_2\}$ , and  $\vec{R}_3 = \{R_3, 0, 0\}$ . Because we used the rigid rotor model, the lengths of the HD and  $H_2$  molecules are fixed at equilibrium values, e.g.,  $R_1=0.7631$  a.u. and  $R_2=0.7668$  a.u., thus leaving us with four free variables. We replace one hydrogen atom H with a deuterium atom D, thus shifting the c.m. of one  $H_2$  molecule to another point, that is from  $O$  to  $O'$ . The length of the vector  $\vec{x}$  is  $x = |\vec{R}_1|/6$ . This is seen in Fig. 16. Then we shift the original coordinate system  $OXYZ$  along the vector  $\vec{R}_1$  to the new one  $O'X'Y'Z'$ . The origin of the new system, i.e.  $O'$ , lies on the c.m. of HD. A new Jacobi vector  $\vec{R}'_3$  is defined connecting the c.m.'s of the HD and  $H_2$  molecules. The new intermolecular distance between HD and  $H_2$  is:

$$R'_3 = \sqrt{R_3^2 + x^2 - 2xR_3 \cos \theta_1}. \quad (14)$$

Now, if we rotate  $O'X'Y'Z'$  around its  $O'Y'$  axis in such a way that the  $OZ'$  axis is directed over the vector  $\vec{R}'_3$  we obtain a new coordinate system  $O'X''Y''Z''$  which should be well designed to carry out computations for the HD+ $H_2$  collision. The rotational angle  $\eta$  satisfies:

$$\cos \eta = \frac{R_3'^2 + R_3^2 - x^2}{2R_3'R_3} \quad (15)$$

$$\sin \eta = \frac{x}{R_3' \sin \theta_1} \quad (16)$$

This transformation converts the initial Jacobi vectors in  $OXYZ$ :  $\vec{R}_1 = \{R_1, \theta_1, 0\}$ ,  $\vec{R}_2 = \{R_2, \theta_2, \varphi_2\}$  and  $\vec{R}_3 = \{R_3, 0, 0\}$  to the corresponding Jacobi vectors with new coordinates in the new  $O'X'Y'Z'$ :  $\vec{R}'_1 = \{R'_1, \theta'_1, \varphi'_2\}$ ,  $\vec{R}'_2 = \{R'_2, \theta'_2, 0\}$  and  $\vec{R}'_3 = \{R'_3, 0, 0\}$ .

The coordinate transformations from  $OXYZ$  to  $O''X''Y''Z''$  changes the original Hinde's PES to the new HD- $H_2$  PES. Rotation of the coordinate system from  $O'X'Y'Z'$  to  $O'X''Y''Z''$  results in a corresponding transformation of the coordinates of the 4-body system as well as changing the distance between the two molecules. One then has the following relations

between new and old variables<sup>36</sup>:

$$\theta'_1 = \arccos(\cos \theta_1 \cos \eta + \sin \theta_1 \sin \eta), \quad (17)$$

$$\theta'_2 = \arccos(\cos \theta_2 \cos \eta + \sin \theta_2 \sin \eta \cos \Phi_2), \quad (18)$$

$$\varphi'_2 = \arccos \left( \cot \phi_2 \cos \eta + \frac{\cot \theta_1 \sin \eta}{\sin \phi_2} \right). \quad (19)$$

In the calculation of HD+H<sub>2</sub> with Hinde's PES one has to use new coordinates  $\theta'_1, \theta'_2, \varphi'_2, R'_3$ . However, the original potential has been expressed through the initial H<sub>2</sub>-H<sub>2</sub> variables, i.e.  $\theta_1, \theta_2, \Phi_2$  and  $R_3$ . Hence they have to be transformed using (17)-(19). Therefore, in the case of the non-symmetrical HD+H<sub>2</sub> collision one should use the formulas (17)-(19) together with (15)-(16) and the expression (14) for the new distance  $R'_3$  between the center of masses of the H<sub>2</sub> and HD molecules.

In general, any consideration of the HD+H<sub>2</sub>, D<sub>2</sub>+HD or D<sub>2</sub>+D<sub>2</sub> systems should begin with the original H<sub>2</sub>-H<sub>2</sub> PES. This six-dimensional function comprises a symmetrical surface over the  $OZ$  coordinate axis. This is shown in Figs. 1 and 16. In spherical coordinates the surface can be described by six variables:  $R_1, \theta_1, R_2, \theta_2, R_3$ , and  $\varphi_2$ . The variables are also shown in the figures. The H<sub>2</sub>-H<sub>2</sub> PES was obtained in the framework of the Born-Oppenheimer model<sup>33</sup> and can be considered as a symmetrical interaction field. When considering non-reactive scattering problems with participation of hydrogen molecules one needs to solve the Schrödinger Eq. (2) with the H<sub>2</sub>-H<sub>2</sub> potential  $V(\vec{R}_1, \vec{R}_2, \vec{R}_3)$ . The solution/propagation runs over the  $\vec{R}_3$  Jacobi vector (please see Fig. 16). Therefore, in the case of the symmetrical H<sub>2</sub>+H<sub>2</sub> and D<sub>2</sub>+D<sub>2</sub> collisions one can use the original H<sub>2</sub>-H<sub>2</sub> PES as it is, i.e. without transformations.

However, in the case of the non-symmetrical (or symmetry-broken) HD+H<sub>2</sub>/D<sub>2</sub> or HD+HD scattering systems one should also apply the original H<sub>2</sub>-H<sub>2</sub> interaction field (PES), but the propagation (solution) of the Schrödinger equation runs, in this case, over the corrected Jacobi vector  $\vec{R}'_3$  which is directed over the new  $OZ''$  axis, as is shown in Fig. 16.

## VI. APPENDIX B: HD+*o*-/*p*-H<sub>2</sub> THERMAL RATE COEFFICIENTS

New data for the thermal rate coefficients,  $k_{j_1 j_2 \rightarrow j'_1 j'_2}(T)$ , Eq. (4), are listed below. The results are obtained with the modified Hinde H<sub>2</sub>-H<sub>2</sub> PES<sup>5</sup>: Table II includes  $k_{j_1 j_2 \rightarrow j'_1 j'_2}(T)$  at

low temperatures for the HD + *para*-H<sub>2</sub> rotational energy transfer collisions and Table III the same information for the HD + *ortho*-H<sub>2</sub> case. The astrophysical HD-cooling function can be computed with the use of formula (13).

## REFERENCES

- <sup>1</sup>P. Diep and J.K. Johnson, *J. Chem. Phys.* **112**, 4465 (2000).
- <sup>2</sup>A.I. Boothroyd, P.G. Martin, W.J. Keogh, and M.J. Peterson, *J. Chem. Phys.* **116**, 666 (2002).
- <sup>3</sup>D. W. Schwenke, *J. Chem. Phys.* **89**, 2076 (1988).
- <sup>4</sup>J. L. Belof, A. C. Stern, and B. Space, *J. Chem. Theory Comput.*, **4** (8), 1332 (2008).
- <sup>5</sup>R.J. Hinde, *J. Chem. Phys.* **128**, 154308 (2008).
- <sup>6</sup>K. Patkowski, W. Cencek, P. Jankowski, K. Szalewicz, J.B. Mehl, G. Garberoglio, A.H. Harvey, *J. Chem. Phys.* **129**, 094304 (2008).
- <sup>7</sup>L. Spitzer, *Physical Processes in the Interstellar Medium*, (Wiley, New York, 1978).
- <sup>8</sup>M. Signore, D. Puy, *Europ. Phys. J. C* **59**, 117 (2009).
- <sup>9</sup>I. D. McGreer and G. L. Bryan, *Astrophys. J.* **685**, 8 (2008).
- <sup>10</sup>D. A. Varshalovich and V. K. Khersonskii, *Sov. Astron. Lett.* **2**, 227 (1976).
- <sup>11</sup>J. Schaefer, *Astron. Astrophys. Suppl. Ser.* **85**, 1101 (1990).
- <sup>12</sup>D.R. Flower, J. Le Bourlot, G. Pineau Des Forets, E. Roueff, *Mon. Not. R. Astron. Soc.* **314**, 753 (2000).
- <sup>13</sup>D. R. Flower, *J. Phys. B* **32**, 1755 (1999).
- <sup>14</sup>S.-I. Chu, *J. Chem. Phys.* **62**, 4089 (1975).
- <sup>15</sup>A. Dalgarno and R. McCray, *Ann. Rev. Astron. Astrophys.* **10**, 375 (1972).
- <sup>16</sup>G. Zarur and H. Rabitz, *J. Chem. Phys.* **60**, 2057 (1974).
- <sup>17</sup>S. Green, *J. Chem. Phys.* **62**, 2271 (1975).
- <sup>18</sup>R. A. Sultanov and D. Guster, *Chem. Phys. Lett.* **436**, 19 (2007).
- <sup>19</sup>R. A. Sultanov, A. V. Khugaev, and D. Guster, *Chem. Phys. Lett.* **475**, 175 (2009).
- <sup>20</sup>R. A. Sultanov and D. Guster, *Chem. Phys.* **326**, 641 (2006); *Chem. Phys. Lett.* **428**, 227 (2006).
- <sup>21</sup>R.A. Sultanov, D. Guster, and S.K. Adhikari, *AIP Advances* **2**, 099 (2012).
- <sup>22</sup>S.K. Pogrebnya and D.C. Clary, *Chem. Phys. Lett.* **363**, 523 (2002).

- <sup>23</sup>S.Y. Lin and H. Guo, Chem. Phys. **289**, 191 (2003).
- <sup>24</sup>F. Gatti, F. Otto, S. Sukiasyan, and H.-D. Meyer, J. Chem. Phys. **123**, 174311 (2005).
- <sup>25</sup>S. Montero and J. Pérez-Ríos, J. Chem. Phys. **141**, 114301 (2014).
- <sup>26</sup>G. Quéméner, N. Balakrishnan, and R. V. Krems, Phys. Rev. A **77**, 030704 (2008).
- <sup>27</sup>W. R. Gentry and C. F. Giese, Phys. Rev. Lett. **39**, 1259 (1977).
- <sup>28</sup>R. A. Sultanov, D. Guster, and S. K. Adhikari, Phys. Rev. A **85**, 052702 (2012).
- <sup>29</sup>D.L. Johnson, R.S. Grace, and J.G. Skofronick, J. Chem. Phys. **71**, 4554 (1979).
- <sup>30</sup>D.W. Chandler and R.L. Farrow, J. Chem. Phys. **85**, 810 (1986).
- <sup>31</sup>R.L. Farrow and D.W. Chandler, J. Chem. Phys. **89**, 1994 (1988).
- <sup>32</sup>B. Maté, F. Thibault, G. Tejeda, J. M. Fernández, and S. Montero, J. Chem. Phys. **122**, 064313 (2005).
- <sup>33</sup>M. Born and R. Oppenheimer, Ann. Phys. **84**, 457 (1927).
- <sup>34</sup>J. M. Hutson and S. Green, *MOLSCAT Computer Code version 14*, (Distributed by Collaborative Comp. Proj. 6 of the Engineering and Physical Sciences Research Council, Daresbury Lab., 1994).
- <sup>35</sup>D. E. Manolopoulos, J. Chem. Phys. **85**, 6425 (1986).
- <sup>36</sup>D. A. Varshalovich, A. N. Moskalev, and V. K. Khersonskii, Quantum Theory of Angular Momentum, Chapter 1.4, p.p. 21-23, (World Scientific, Singapore, 1988).
- <sup>37</sup>L. Machin and E. Roueff, A&A **460**, 953 (2006).
- <sup>38</sup>M. P. Hodges and R. J. Wheatley, J. Chem. Phys. **114**, 8836 (2001).
- <sup>39</sup>D. Hollenbach and C.F. McKee, Astrophys. J. Suppl. Ser. **41**, 555 (1979).
- <sup>40</sup>D. Galli and F. Palla, Planet. Space Sci. **50**, 1197 (2002).
- <sup>41</sup>A. Lipovka, R. Nunez-Lopez, and V. Avila-Reese, Mon. Not. R. Astron. Soc. **361**, 850 (2005).
- <sup>42</sup>C.M. Coppola, L. Lodi, and J. Tennyson, Mon. Not. R. Astron. Soc. **415**, 487 (2011).
- <sup>43</sup>A.I. Boothroyd, W.K. Keogh, P.G. Martin, and M.R. Peterson, J. Chem. Phys. **95**, 4343 (1991); A.I. Boothroyd, J. Chem. Phys. **104**, 7139 (1996).
- <sup>44</sup>Y.-S. M. Wu, A. Kuppermann, J.B. Anderson, Phys. Chem. Chem. Phys. **1**, 929 (1999).

TABLE I. Total rotational energy  $\mathcal{E}_{rot}$  in the four-atomic system: HD( $j_1$ )+ $p$ -H<sub>2</sub>( $j_2$ ) and HD( $j_1$ )+ $o$ -H<sub>2</sub>( $j_2$ ). Here,  $\mathcal{E}_{rot} = B_1 j_1(j_1 + 1) + B_2 j_2(j_2 + 1)$ , where  $B_{1(2)}$  are the rotational constants of rigid rotors  $ab$  and  $cd$  respectively.

$\mathcal{E}_{rot}$ (cm <sup>-1</sup> )	HD( $j_1$ )	$p$ -H <sub>2</sub> ( $j_2$ )	$\mathcal{E}_{rot}$ (cm <sup>-1</sup> )	HD( $j_1$ )	$o$ -H <sub>2</sub> ( $j_2$ )
0.0	0	0	121.6	0	1
89.4	1	0	211.0	1	1
268.2	2	0	389.8	2	1
364.8	0	2	658.0	3	1
454.2	1	2	729.6	0	3
536.4	3	0	819.0	1	3
633.0	2	2	997.8	2	3



TABLE II. Low temperature rotational de-excitation thermal rate coefficients  $k_{ij \rightarrow i'j'}(T)$  in the  $\text{HD}(i) + \text{para-H}_2(j) \rightarrow \text{HD}(i') + \text{para-H}_2(j')$  collision. All results are multiplied by a constant value  $\alpha = 10^{11}$ . The data are in the unit  $\text{cm}^3 \text{sec}^{-1}$ .

$T(\text{K})$	10-00	20-10	20-00	02-20	02-10	02-00	12-02	12-20	12-10	12-00
2	4.774	6.892	1.115	0.914	3.88E-02	2.45E-03	4.960	2.22E-02	5.61E-03	6.01E-04
4	4.099	4.817	0.670	0.553	2.31E-02	1.46E-03	4.194	1.74E-02	4.40E-03	4.56E-04
6	3.780	4.007	0.485	0.444	1.83E-02	1.16E-03	3.841	1.55E-02	3.96E-03	4.04E-04
8	3.574	3.580	0.390	0.393	1.60E-02	1.01E-03	3.617	1.44E-02	3.74E-03	3.76E-04
10	3.431	3.321	0.335	0.363	1.47E-02	9.26E-04	3.464	1.38E-02	3.61E-03	3.60E-04
12	3.329	3.153	0.299	0.345	1.39E-02	8.74E-04	3.356	1.33E-02	3.54E-03	3.51E-04
14	3.256	3.039	0.274	0.333	1.34E-02	8.39E-04	3.278	1.31E-02	3.51E-03	3.45E-04
16	3.203	2.960	0.257	0.325	1.31E-02	8.17E-04	3.223	1.29E-02	3.50E-03	3.43E-04
18	3.166	2.907	0.245	0.319	1.29E-02	8.03E-04	3.183	1.29E-02	3.50E-03	3.41E-04
20	3.140	2.872	0.236	0.315	1.27E-02	7.94E-04	3.157	1.32E-02	3.52E-03	3.41E-04
22	3.125	2.850	0.229	0.313	1.27E-02	7.91E-04	3.140	1.41E-02	3.54E-03	3.43E-04
24	3.116	2.839	0.224	0.311	1.27E-02	7.91E-04	3.131	1.63E-02	3.57E-03	3.47E-04
26	3.114	2.836	0.221	0.310	1.28E-02	7.94E-04	3.129	2.04E-02	3.62E-03	3.53E-04
30	3.124	2.848	0.217	0.310	1.30E-02	8.06E-04	3.141	3.84E-02	3.82E-03	3.82E-04
40	3.204	2.948	0.218	0.313	1.39E-02	8.66E-04	3.228	1.78E-01	5.29E-03	6.11E-04
50	3.327	3.102	0.227	0.319	1.51E-02	9.48E-04	3.360	4.83E-01	8.52E-03	1.12E-03
60	3.474	3.283	0.241	0.325	1.64E-02	1.05E-03	3.512	9.10E-01	1.32E-02	1.84E-03
80	3.798	3.687	0.275	0.335	1.93E-02	1.27E-03	3.841	1.86E+00	2.39E-02	3.49E-03
100	4.137	4.115	0.315	0.342	2.24E-02	1.52E-03	4.178	2.66E+00	3.34E-02	4.95E-03
120	4.478	4.549	0.359	0.347	2.54E-02	1.81E-03	4.514	3.21E+00	4.07E-02	6.05E-03
140	4.815	4.982	0.405	0.351	2.85E-02	2.11E-03	4.844	3.54E+00	4.59E-02	6.82E-03
160	5.145	5.410	0.452	0.353	3.16E-02	2.45E-03	5.168	3.72E+00	4.95E-02	7.35E-03
180	5.469	5.830	0.500	0.354	3.47E-02	2.80E-03	5.485	3.78E+00	5.20E-02	7.72E-03
200	5.783	6.241	0.550	0.354	3.77E-02	3.17E-03	5.793	3.77E+00	5.38E-02	7.99E-03
250	6.528	7.218	0.674	0.352	4.50E-02	4.18E-03	6.525	3.58E+00	5.65E-02	8.45E-03
300	7.204	8.114	0.796	0.349	5.18E-02	5.23E-03	7.193	3.29E+00	5.81E-02	8.81E-03

TABLE III. Low temperature rotational de-excitation thermal rate coefficients  $k_{ij \rightarrow i'j'}(T)$  in the  $\text{HD}(i) + \text{ortho-H}_2(j) \rightarrow \text{HD}(i') + \text{ortho-H}_2(j')$  collision. All results are multiplied by a constant value  $\alpha = 10^{11}$ . The data are in the unit  $\text{cm}^3 \text{sec}^{-1}$ .

$T(\text{K})$	11-01	21-11	21-01	31-21	31-11	31-01	03-21	03-11	03-31	13-03	13-31
2	4.921	4.903	0.322	3.691	0.299	3.68E-02	6.98E-02	7.74E-03	2.16E-03	5.037	1.50E-01
4	4.189	3.807	0.256	2.669	0.218	2.69E-02	3.90E-02	4.30E-03	1.20E-03	4.222	1.10E-01
6	3.844	3.383	0.229	2.304	0.189	2.33E-02	2.99E-02	3.28E-03	9.19E-04	3.855	9.58E-02
8	3.623	3.146	0.214	2.112	0.173	2.14E-02	2.57E-02	2.80E-03	7.94E-04	3.625	8.88E-02
10	3.472	2.997	0.204	1.996	0.164	2.03E-02	2.34E-02	2.54E-03	7.31E-04	3.469	8.48E-02
12	3.364	2.898	0.198	1.922	0.158	1.96E-02	2.20E-02	2.38E-03	7.00E-04	3.359	8.24E-02
14	3.287	2.831	0.194	1.874	0.154	1.91E-02	2.12E-02	2.28E-03	6.92E-04	3.280	8.10E-02
16	3.231	2.787	0.191	1.843	0.152	1.88E-02	2.07E-02	2.22E-03	7.02E-04	3.223	8.03E-02
18	3.192	2.759	0.189	1.825	0.151	1.87E-02	2.04E-02	2.18E-03	7.30E-04	3.183	8.00E-02
20	3.164	2.743	0.189	1.816	0.150	1.87E-02	2.03E-02	2.17E-03	7.77E-04	3.155	8.00E-02
22	3.147	2.737	0.189	1.814	0.150	1.87E-02	2.03E-02	2.16E-03	8.42E-04	3.137	8.04E-02
24	3.138	2.737	0.189	1.817	0.151	1.88E-02	2.04E-02	2.17E-03	9.26E-04	3.127	8.09E-02
26	3.134	2.744	0.190	1.826	0.152	1.89E-02	2.06E-02	2.19E-03	1.03E-03	3.124	8.16E-02
30	3.143	2.772	0.193	1.853	0.155	1.94E-02	2.11E-02	2.25E-03	1.28E-03	3.131	8.33E-02
40	3.220	2.895	0.205	1.962	0.166	2.10E-02	2.30E-02	2.47E-03	2.12E-03	3.207	8.87E-02
50	3.343	3.060	0.220	2.105	0.181	2.31E-02	2.54E-02	2.78E-03	3.13E-03	3.328	9.50E-02
60	3.488	3.249	0.238	2.269	0.199	2.56E-02	2.80E-02	3.14E-03	4.19E-03	3.471	1.02E-01
80	3.811	3.661	0.279	2.634	0.240	3.16E-02	3.35E-02	3.98E-03	6.40E-03	3.792	1.14E-01
100	4.150	4.094	0.323	3.028	0.287	3.88E-02	3.92E-02	4.96E-03	8.72E-03	4.127	1.26E-01
120	4.490	4.532	0.370	3.440	0.339	4.69E-02	4.50E-02	6.07E-03	1.12E-02	4.465	1.37E-01
140	4.827	4.969	0.419	3.864	0.396	5.60E-02	5.08E-02	7.28E-03	1.38E-02	4.799	1.46E-01
160	5.157	5.400	0.470	4.295	0.457	6.60E-02	5.66E-02	8.58E-03	1.65E-02	5.127	1.55E-01
180	5.480	5.824	0.521	4.731	0.521	7.69E-02	6.24E-02	9.97E-03	1.93E-02	5.447	1.62E-01
200	5.795	6.238	0.573	5.169	0.589	8.87E-02	6.80E-02	1.14E-02	2.22E-02	5.759	1.69E-01
250	6.539	7.224	0.704	6.258	0.772	1.21E-01	8.14E-02	1.53E-02	2.98E-02	6.498	1.82E-01
300	7.215	8.127	0.831	7.311	0.964	1.57E-01	9.37E-02	1.93E-02	3.73E-02	7.171	1.92E-01

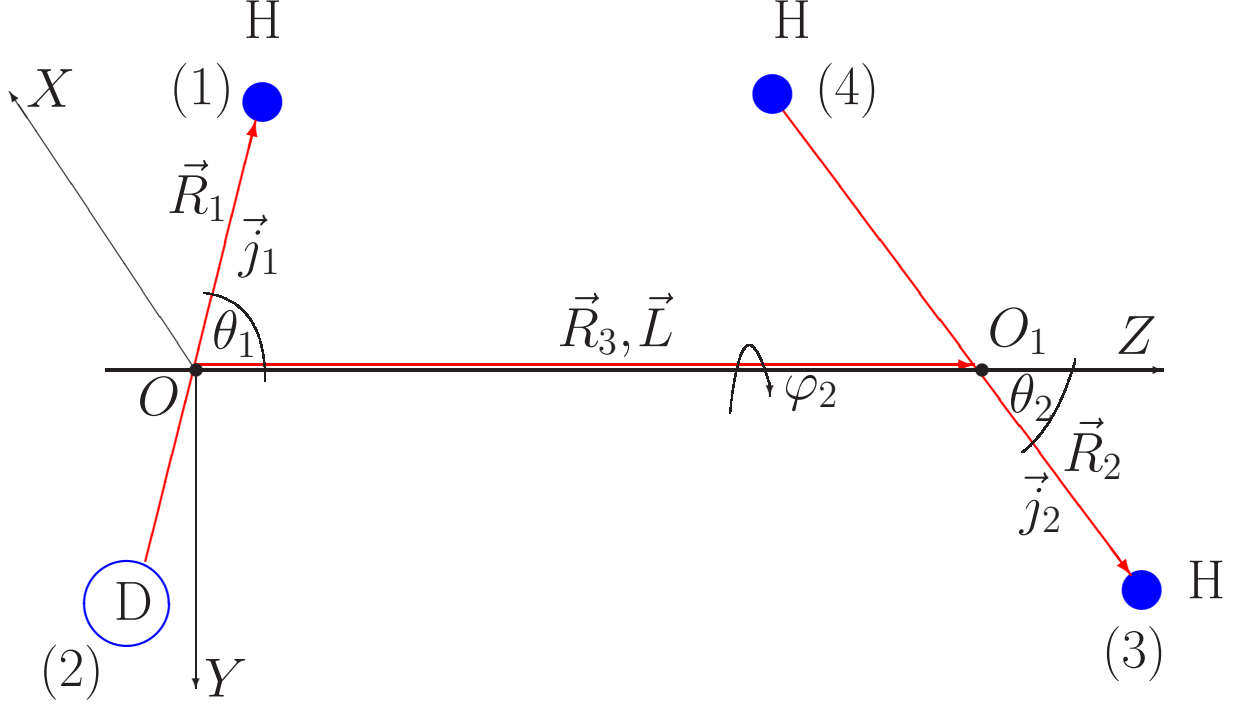


FIG. 1. (Color online) Four-atomic system (12)+(34) or HD+H<sub>2</sub>. Here, H is a hydrogen atom and D is deuterium, represented by the few-body Jacobi coordinates:  $\vec{R}_1$ ,  $\vec{R}_2$  and  $\vec{R}_3$ . The vector  $\vec{R}_3$  connects the center of masses of the HD and H<sub>2</sub> molecules, i.e.  $O$  and  $O_1$  respectively, and is directed over the axis  $OZ$ ,  $\theta_1$  is the angle between  $\vec{R}_1$  and  $\vec{R}_3$ ,  $\theta_2$  is the angle between  $\vec{R}_2$  and  $\vec{R}_3$ ,  $\varphi_2$  is the torsional angle,  $\vec{j}_1$ ,  $\vec{j}_2$  and  $\vec{L}$  are quantum angular momenta over the corresponding Jacobi coordinates  $\vec{R}_1$ ,  $\vec{R}_2$  and  $\vec{R}_3$ .

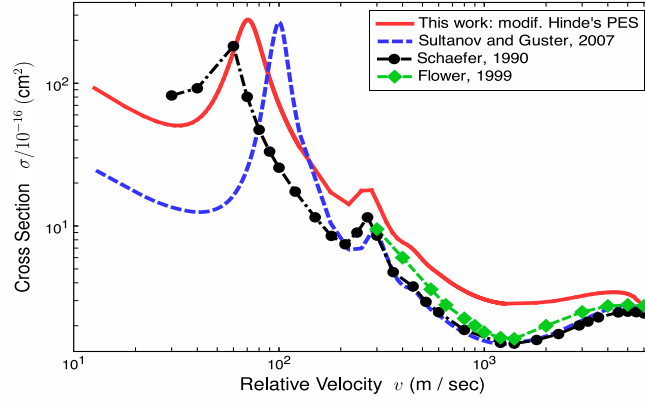


FIG. 2. (Color online) The total cross section of the HD(1) + H<sub>2</sub>(0) → HD(0) + H<sub>2</sub>(0) inelastic rotational energy transfer collision. The numbers in the brackets are the rotational quantum numbers of the corresponding two-atomic molecules.

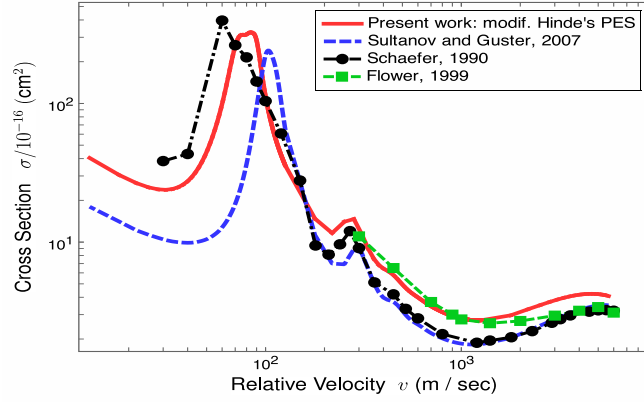


FIG. 3. (Color online) The total cross section of the HD(2) + H<sub>2</sub>(0) → HD(1) + H<sub>2</sub>(0) inelastic rotational energy transfer collision. The numbers in the brackets are the rotational quantum numbers of the corresponding two-atomic molecules.

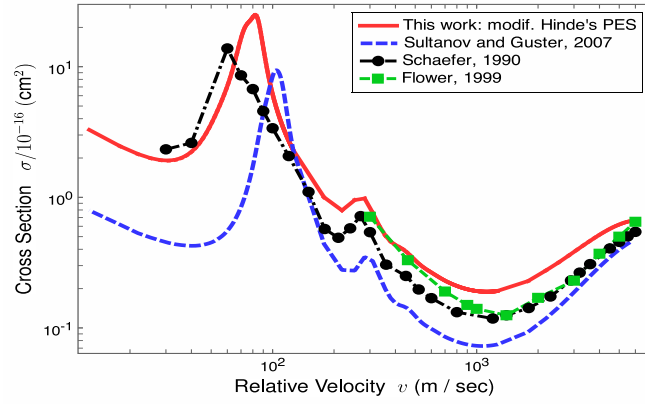


FIG. 4. (Color online) The total cross section of the HD(2) + H<sub>2</sub>(0) → HD(0) + H<sub>2</sub>(0) inelastic rotational energy transfer collision. The numbers in the brackets are the rotational quantum numbers of the corresponding two-atomic molecules.

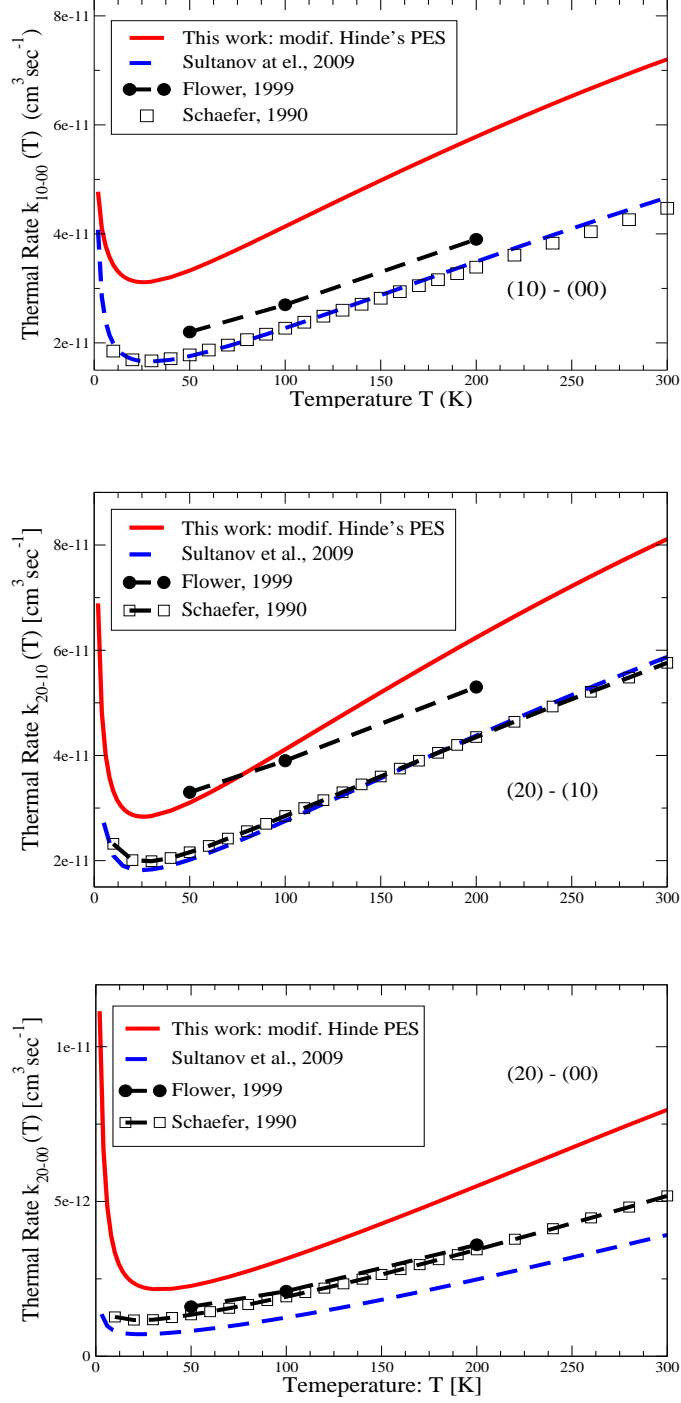


FIG. 5. (Color online) Upper plot: the rotational de-excitation thermal rate coefficients  $k_{ij \rightarrow i'j'}(T)$  for the  $\text{HD}(1) + \text{H}_2(0) \rightarrow \text{HD}(0) + \text{H}_2(0)$  collision. Middle and lower plots represent  $k_{ij \rightarrow i'j'}(T)$  for the  $\text{HD}(2) + \text{H}_2(0) \rightarrow \text{HD}(1) + \text{H}_2(0)$  and  $\text{HD}(2) + \text{H}_2(0) \rightarrow \text{HD}(0) + \text{H}_2(0)$  channels correspondingly.

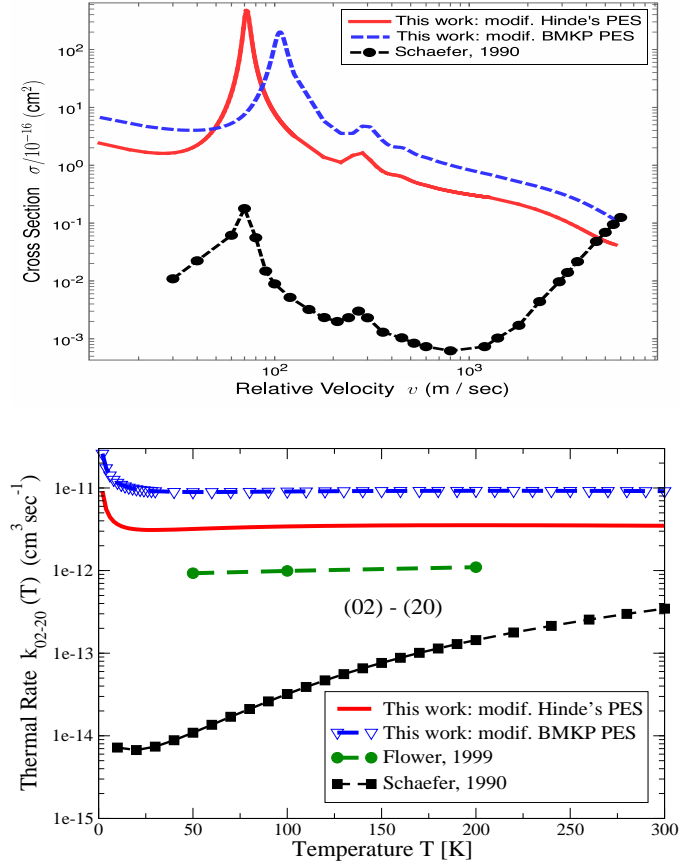


FIG. 6. (Color online) Upper plot: the total cross section of the  $\text{HD}(0) + \text{H}_2(2) \rightarrow \text{HD}(2) + \text{H}_2(0)$  inelastic rotational energy transfer collision. The numbers in the brackets are the rotational quantum numbers of the corresponding two-atomic molecules. Lower plot: the corresponding thermal rate coefficient, i.e. the process (02)-(20).



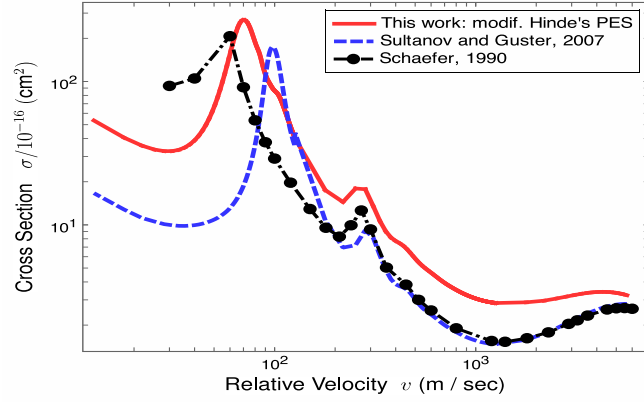


FIG. 7. (Color online) The total cross section (upper plot) and thermal rate coefficients (lower plot) of the HD(1) + H<sub>2</sub>(2) → HD(0) + H<sub>2</sub>(2) inelastic rotational energy transfer collision. The numbers in the brackets are the rotational quantum numbers of the corresponding two-atomic molecules.

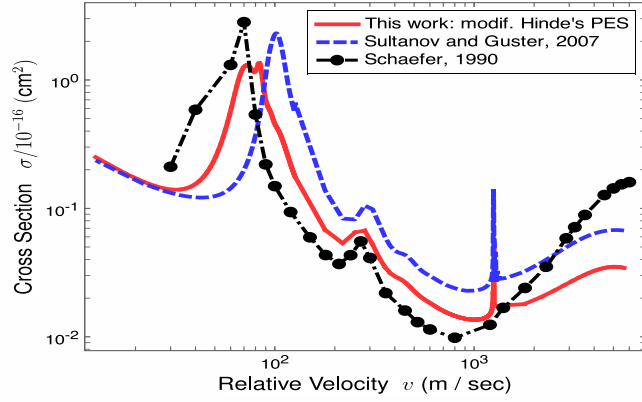


FIG. 8. (Color online) The total cross section of the  $\text{HD}(1) + \text{H}_2(2) \rightarrow \text{HD}(2) + \text{H}_2(0)$  inelastic rotational energy transfer collision. The numbers in the brackets are the rotational quantum numbers of the corresponding two-atomic molecules.

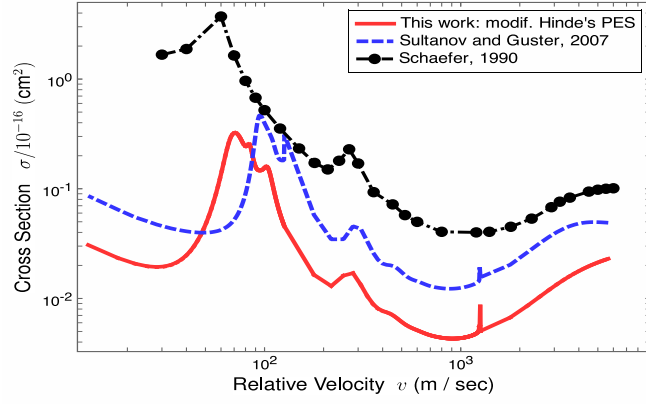


FIG. 9. (Color online) The total cross section of the HD(1) + H<sub>2</sub>(2) → HD(1) + H<sub>2</sub>(0) inelastic rotational energy transfer collision. The numbers in the brackets are the rotational quantum numbers of the corresponding two-atomic molecules.

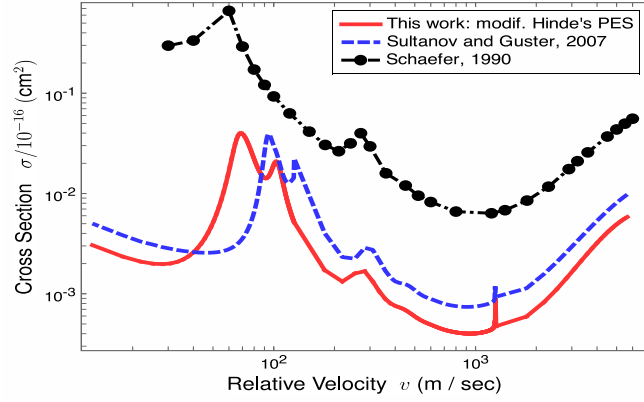


FIG. 10. (Color online) The total cross section of the  $\text{HD}(1) + \text{H}_2(2) \rightarrow \text{HD}(0) + \text{H}_2(0)$  inelastic rotational energy transfer collision. The numbers in the brackets are the rotational quantum numbers of the corresponding two-atomic molecules.

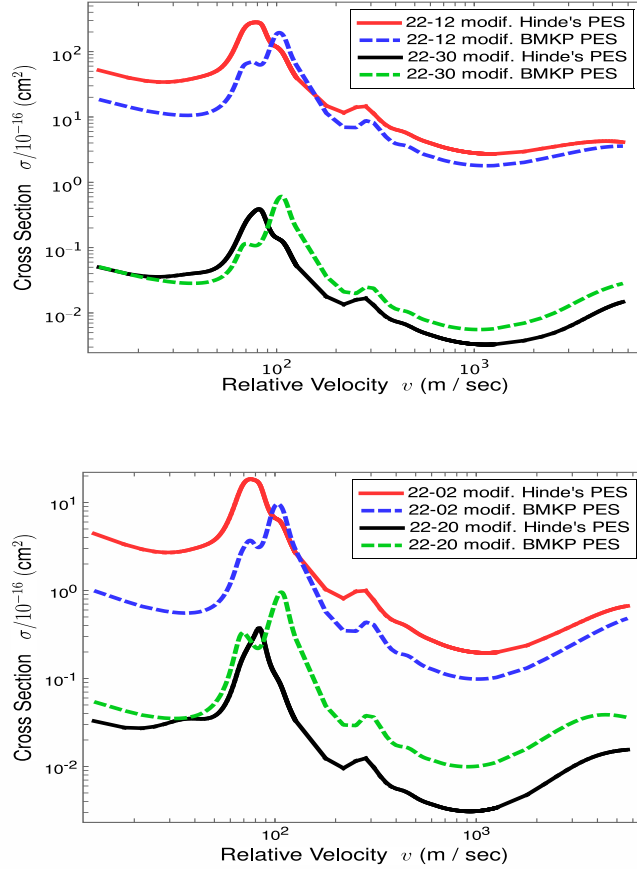


FIG. 11. (Color online) Upper graph: the total cross sections of the HD(2) + H<sub>2</sub>(2) → HD(1) + H<sub>2</sub>(2) and HD(2) + H<sub>2</sub>(2) → HD(3) + H<sub>2</sub>(0) inelastic rotational energy transfer collisions. Lower graph: the total cross sections of the HD(2) + H<sub>2</sub>(2) → HD(0) + H<sub>2</sub>(2) and HD(2) + H<sub>2</sub>(2) → HD(2) + H<sub>2</sub>(0) inelastic rotational energy transfer collisions. The numbers in the brackets are the rotational quantum numbers of the corresponding two-atomic molecules. Results are obtained with two different PESs.

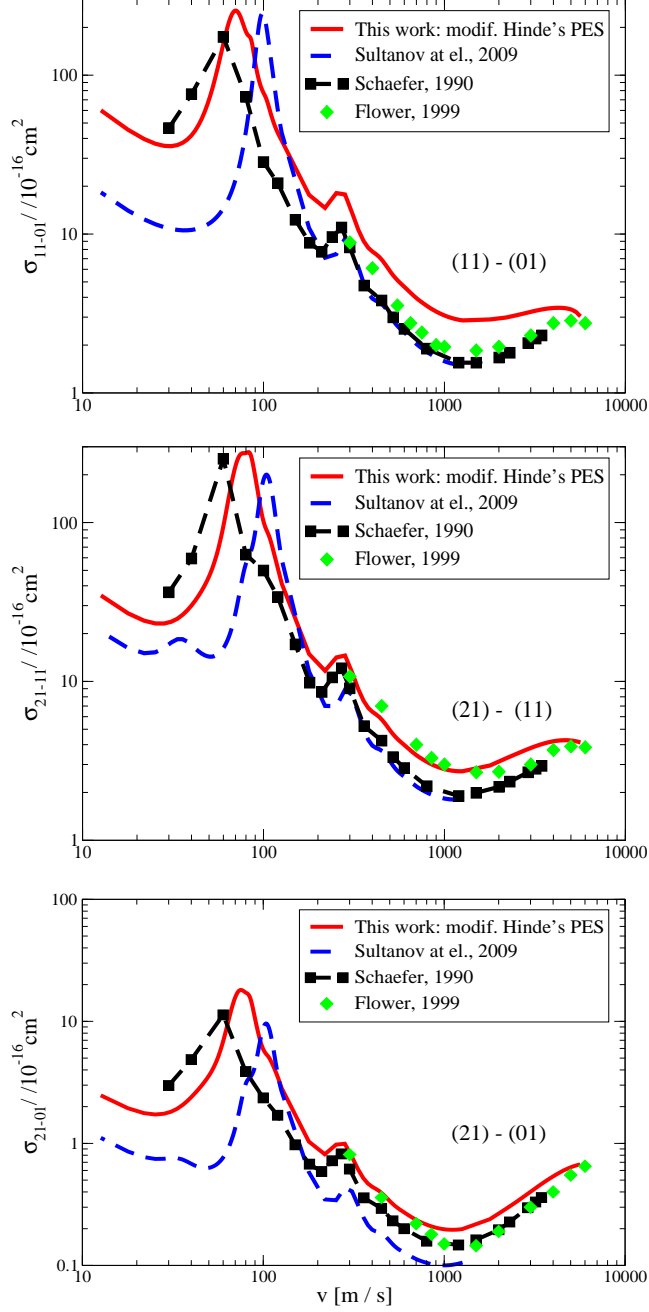


FIG. 12. (Color online) The HD+*ortho*-H<sub>2</sub> case. Upper plot: the total cross section of the HD(1) + H<sub>2</sub>(1) → HD(0) + H<sub>2</sub>(1) inelastic rotational energy transfer collision. Middle and lower plots represent the following two integral cross sections: HD(2) + H<sub>2</sub>(1) → HD(1) + H<sub>2</sub>(1) and HD(2) + H<sub>2</sub>(1) → HD(0) + H<sub>2</sub>(1) correspondingly. The numbers in the brackets are the rotational quantum numbers of the corresponding two-atomic molecules.

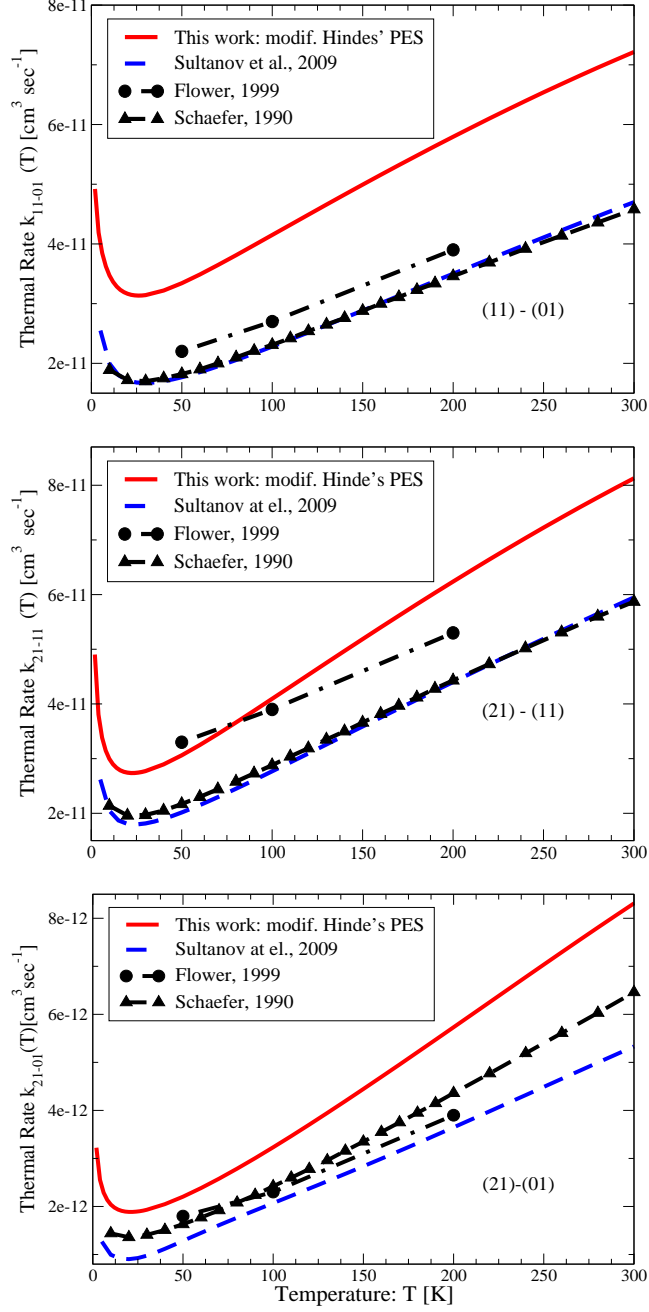


FIG. 13. (Color online) The HD+*ortho*-H<sub>2</sub> case. Upper plot: the rotational de-excitation thermal rate coefficients  $k_{ij \rightarrow i'j'}(T)$  for the HD(1) + H<sub>2</sub>(1)  $\rightarrow$  HD(0) + H<sub>2</sub>(1) collision. The middle and lower plots represent  $k_{ij \rightarrow i'j'}(T)$  for the HD(2) + H<sub>2</sub>(1)  $\rightarrow$  HD(1) + H<sub>2</sub>(1) and HD(2) + H<sub>2</sub>(1)  $\rightarrow$  HD(0) + H<sub>2</sub>(1) channels correspondingly.

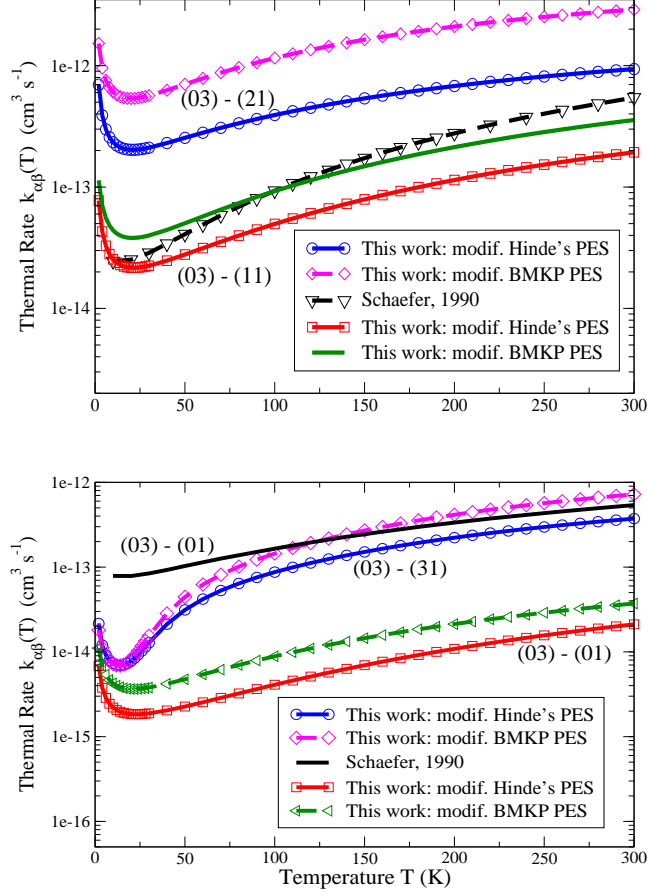


FIG. 14. (Color online) The HD+*ortho*-H<sub>2</sub> case. Upper plot: the rotational de-excitation thermal rate coefficients  $k_{ij \rightarrow i'j'}(T)$  for the HD(0) + H<sub>2</sub>(3)  $\rightarrow$  HD(2) + H<sub>2</sub>(1) and HD(0) + H<sub>2</sub>(3)  $\rightarrow$  HD(1) + H<sub>2</sub>(1) collisions together with the corresponding result from<sup>11</sup>. The lower plot represents  $k_{ij \rightarrow i'j'}(T)$  for the HD(0) + H<sub>2</sub>(3)  $\rightarrow$  HD(3) + H<sub>2</sub>(1) and HD(0) + H<sub>2</sub>(3)  $\rightarrow$  HD(0) + H<sub>2</sub>(1) channels correspondingly. The results of this paper were obtained with the use of the modified Hinde and BMKP PESs.



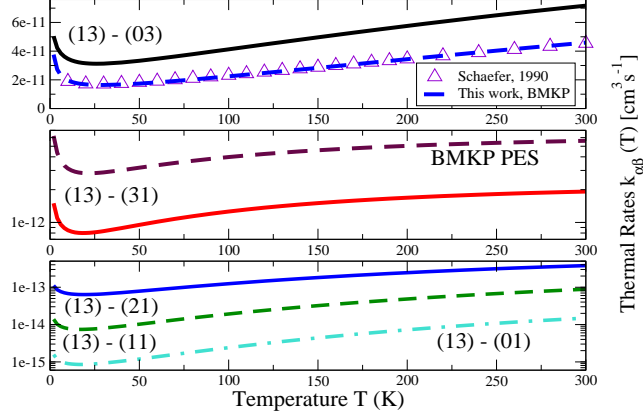


FIG. 15. (Color online) The HD+*ortho*-H<sub>2</sub> case. Upper plot: the rotational de-excitation thermal rate coefficients  $k_{ij \rightarrow i'j'}(T)$  for the HD(1) + H<sub>2</sub>(3) → HD(0) + H<sub>2</sub>(3) collision. The middle plot represents  $k_{ij \rightarrow i'j'}(T)$  for the HD(1) + H<sub>2</sub>(3) → HD(3) + H<sub>2</sub>(1) process, and lower plot shows three results for the HD(1) + H<sub>2</sub>(3) → HD(2) + H<sub>2</sub>(1), HD(1) + H<sub>2</sub>(3) → HD(1) + H<sub>2</sub>(1), and HD(1)+H<sub>2</sub>(3) → HD(0)+H<sub>2</sub>(1) collisions correspondingly. The results of this paper were obtained with the use of the modified Hinde and BMKP PESs.

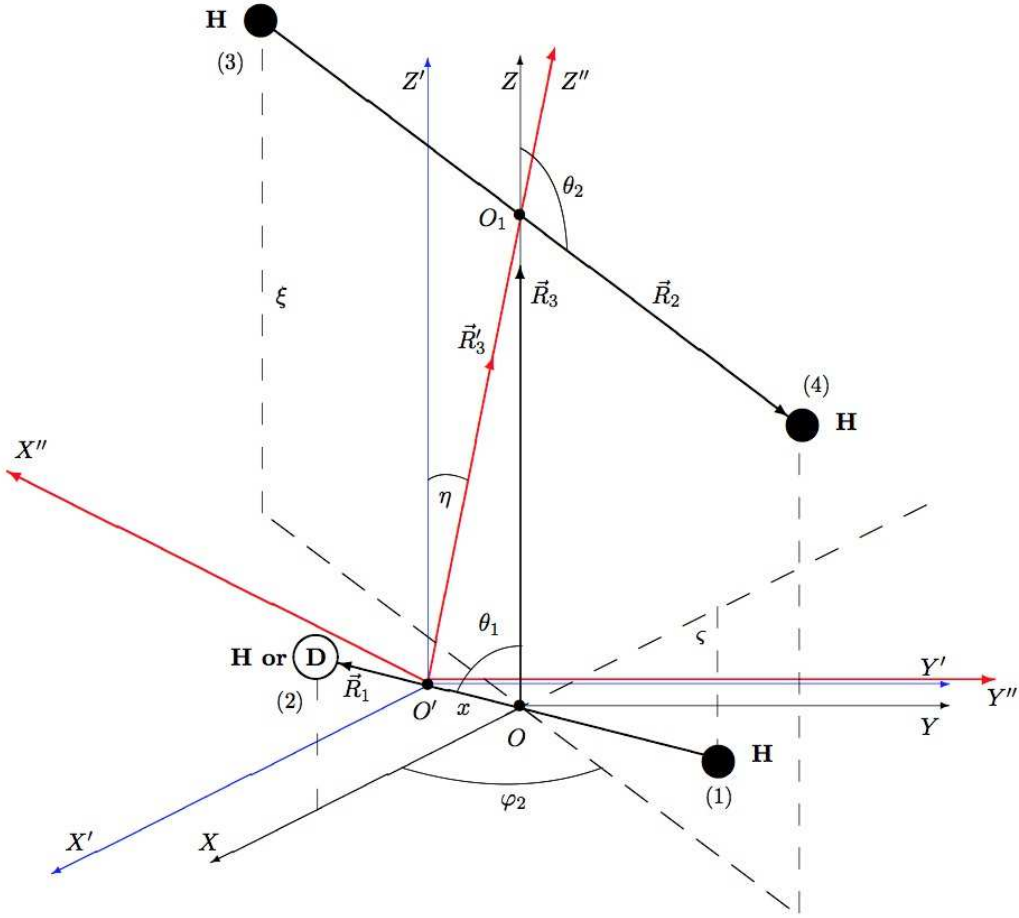


FIG. 16. (Color online) Four-atomic system 1234 or H-D-H-H is shown together with its few-body Jacobi coordinates  $\{\vec{R}_1, \vec{R}_2, \vec{R}_3\}$ . The original cartesian coordinate system is  $OXYZ$ . The center of mass of the original  $H_2$  molecule lies in point  $O$ .  $O'X'Y'Z'$  is a system which was shifted in parallel from the original system,  $O'$  lies in the center of mass of the actual HD molecule. The close-coupling equations are solved using the space-fixed coordinate system  $O'X''Y''Z''$ . The vector  $\vec{R}_3'$  connects the center of masses of the HD and  $H_2$  molecules. HD is the first molecule with a rotational constant  $B_e(1)=44.7 \text{ cm}^{-1}$  and quantum angular momentum of  $j_1$ ,  $H_2$  is the second molecule with rotational constant of  $B_e(2)=60.8 \text{ cm}^{-1}$  and uses momentum  $j_2$  in the system;  $R_1 = 0.7631 \text{ \AA}$  and  $R_2 = 0.7668 \text{ \AA}$  are fixed interatomic distances in each hydrogen molecule HD and  $H_2$  respectively.